Array optimisation for multichannel electrical resistivity tomography instruments

P B Wilkinson, R D Ogilvy, J E Chambers, P I Meldrum and O Kuras. British Geological Survey, Keyworth, Nottingham, NG12 5GG, United Kingdom.

Near Surface 2007

Abstract

In recent years there has been considerable research into the selection of near-optimal arrays of electrode configurations that enhance the resolution of electrical resistivity tomography (ERT) images. Several algorithms have been developed that select resistivity measurements based on their contribution to the cumulative sensitivity of the array (Furman et al., 2004; Hennig and Weller, 2005) or its model resolution matrix (Stummer et al. , 2004; Wilkinson et al., 2006a; 2006b). Homogeneous subsurface resistivity distributions were assumed for these studies, although better results can be obtained using the same algorithms if the resistivity distribution is known a priori (Anthansiou, 2006). When compared to standard arrays, such as dipole-dipole or Wenner-Schlumberger, optimised arrays can substantially improve the resolution of the ERT image for the same number of measurements (Wilkinson et al., 2006b). The driver for researching array optimisation techniques has been the development of computer controlled ERT systems that can address arbitrary combinations of current and potential electrodes. Unfortunately all the published optimisation algorithms share a problem that is likely to impede their wider use: the arrays that they produce are inherently 'single channel' (SC). Since they do not take advantage of the multichannel (MC) capability of modern ERT instruments, the optimised arrays that they produce are rather inefficient to use compared to many standard arrays that are well suited to MC operation. However, we have developed a simple extension that constrains our previous algorithm to choose near-optimal configurations that also fit well into a MC measurement scheme. This extension could easily be adapted to work with the other optimisation schemes cited above.

Our original SC algorithm is described in detail in Wilkinson et al. (2006a), and is based on the work of Stummer et al. (2004). Briefly, we use a linearised approximation of the model resolution matrix **R** to estimate the model resolution $R(j)$, defined as the jth diagonal element of **R**, for each of the m resistivity cells in the image ($1 \leqslant j \leqslant m$). We also define the relative model resolution $R_r(j) = R(j)/R_c(j)$, where R_c is the model resolution of the 'comprehensive' set containing all the electrode configurations that the algorithm can select. As an initial base set, we chose a small array of dipole-dipole configurations with an a-spacing of 5 m (one electrode spacing) and n-levels of $1 \rightarrow 6$. At each iteration of the optimisation procedure, a 'goodness function' is calculated for each unused configuration in the comprehensive set. This tends to rank highly those configurations that would give the greatest improvement to the model resolution. A specified number of the highest ranked configurations are added to the base set at each iteration. To avoid having to update R for every additional configuration, we instead check that the sensitivity distributions of the configurations have at least a given degree of orthogonality to those that have already been added in the same iteration. This is quantified by a maximum limit on their linear dependence, the optimum limit being determined empirically for different conditions (number of electrodes, model size, number of iterations etc).

The SC alorithm selects additional configurations based solely on estimates of their benefit to the model resolution, without considering how to group these configurations together for MC use. Our MC version of the same algorithm is designed for use with any modern ERT instrument that can measure many simultaneous potential differences for a given pair of current electrodes. As a specific example we consider arrays optimised for use with the AGI SuperSting, which is an eight-channel system. We refer to each group of configurations as a 'command', and the desired number of commands, c, is selected before the algorithm runs. The basis of the MC algorithm is identical to the SC version, i.e. the configurations are ranked by goodness and tested for orthogonality. But in addition, the commands are filled with configurations according to the following procedure:

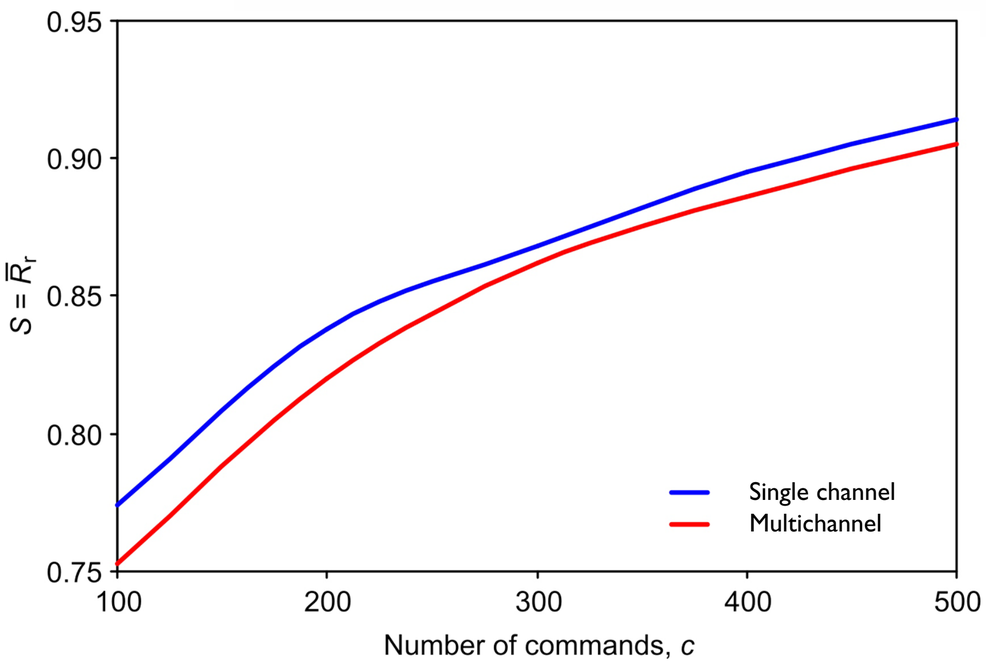

Figure 1 Average model resolution S as a function of number of commands c for SC (blue) and MC (red) algorithms.

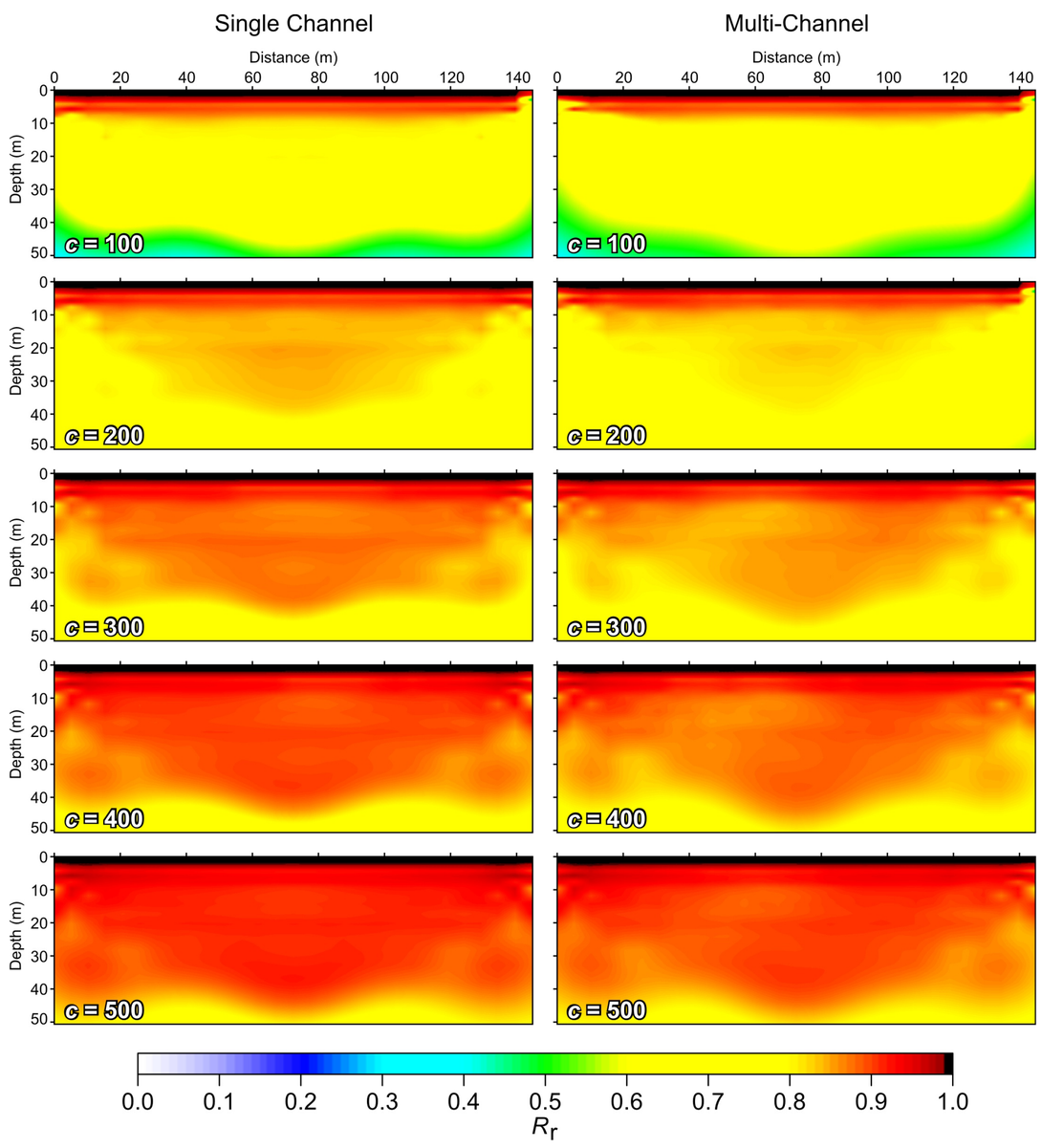

Figure 2 Distribution of the relative model resolution R_r produced by the SC and MC algorithms for the given number of commands, c.

1. If the highest ranked configuration has the same current electrodes as an existing command, *and* one of its potential electrodes is the same as either the first or last potential electrode of the that command, *and* its other potential electrode is not already in use in that command, then add this configuration to that command.

2. If this configuration cannot be added to any existing command, *and* some commands do not yet contain any configurations, then start a new command with this configuration.

3. Otherwise ignore this configuration for this iteration, and proceed to the next highest ranked configuration. Having checked for suitable orthogonality, repeat from Step 1 until the desired number of configurations has been added for this iteration. At this point, recalculate R and the goodness functions, and then repeat from Step 1.

The extra steps involved in grouping the configurations together cause the MC algorithm to be typically 10%-25% slower than the SC algorithm, sometimes requiring a few extra iterations to complete. However, it produces arrays that are nearly as close to optimal as the SC version. This is illustrated by Figure 1 which shows S, the average value of R_r across the whole model space, as a function of the number of commands for the MC and SC algorithm (red and blue lines respectively). Note that $0 \leqslant S \leqslant 1$, where $S = 1$ would be obtained by the comprehensive set containing 51 373 configurations. Both algorithms deliver similar results with $S > 0.9$ for only 500 commands (equivalent to 4000 SC configurations), less than 8% of the total available measurements. The corresponding spatial distributions of R_r produced by the SC and MC algorithms also match very closely (Figure 2).

To test the actual inverted image resolution obtained by the SC and MC optimised arrays, we have used synthetic data generated by the Res2DMod program using a simple forward model comprising four 100 Ωm rectangular prisms (shown by white outlines in Figure 3) embedded in an otherwise homogeneous 10 Ωm half-space. The companion Res2DInv program was used to invert this data using an l_1-norm (robust) model constraint. Figure 3 shows the inverted images and the average resistivities in the areas bounded by the border of each prism. Qualitatively and quantitatively the images obtained by the two versions of the algorithm are extremely similar, showing that the extension to MC operation has been successful, and has not adversely affected the optimisation performance.

In summary, we have enhanced the capability of our optimisation algorithm, enabling it to make full use of multi-channel ERT instruments. The modifications are relatively simple and incur only a small overhead in execution time. The multichannel algorithm produces ERT arrays that are nearly as close to optimal as the original single channel version, with differences in the respective average model resolutions being <5% over a range of array sizes. Collecting near-optimal datasets using a multichannel array is much faster than with an equivalent single channel array; in general the speed is increased by a factor of the number of channels (in our case eight).

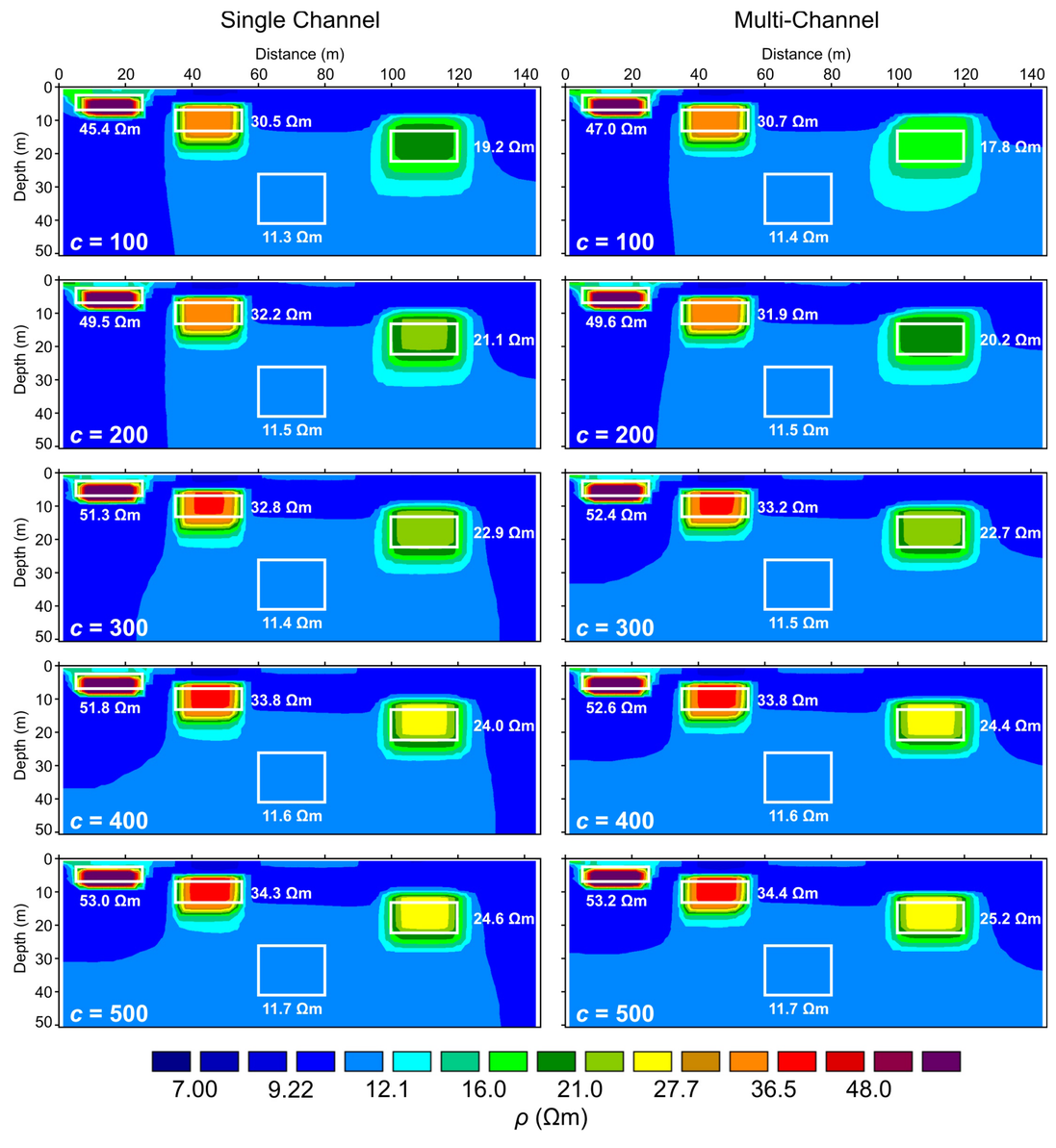

Figure 3 Inverted images obtained from synthetic forward models comprising resistive prisms (100 Ωm, shown as white outlines) embedded in a background half-space of 10 Ωm. Each displayed resistivity value is the average of the inverted image resistivities over the area of the corresponding prism.

Acknowledgements

This paper is published with the permission of the Executive Director of the British Geological Survey (NERC).

References

Anthansiou, E, Tsourlos, P, Papazachos, C B, and Tsokas, G N. 2006 Optimising resistivity array configurations by using a non-homogeneous background model. Proceedings of the 12th meeting of the EAGE Near Surface Geophysics Conference, Helsinki, Finland.

Furman, A, Ferré, T P A, and Warrick, A W. 2004 Optimisation of ERT surveys for monitoring transient hydrological events using perturbation sensitivity and genetic algorithms. *Vadose Zone Journal* 3, 1230-1239.

Hennig, T, and Weller, A. 2005 Two dimensional object orientated focussing of geoelectrical multielectrode measurements. Proceedings of the 11th meeting of the EAGE Near Surface Geophysics Conference, Palermo, Italy.

Stummer, P, Maurer, H, and Green, A G. 2004 Experimental design: Electrical resistivity data sets that provide optimum subsurface information. *Geophysics*, Vol 69, 120-139.

Wilkinson, P B. Meldrum, P I., Chambers, J E, Kuras, O, and Ogilvy, R D. 2006a Improved strategies for the automatic selection of optimised sets of electrical resistivity tomography measurement configurations. *Geophysical Journal International* Vol 167, 1119-1126.

Wilkinson, P B, Kuras, O, Meldrum, P I, Chambers, J E, and Ogilvy, R D. 2006b Comparison of the spatial resolution of standard and optimised electrical resistivity tomography arrays. Proceedings of the 12th meeting of the EAGE Near Surface Geophysics Conference, Helsinki, Finland.

Contact details:
Dr Paul Wilkinson,
Electrical Tomography Programme,
British Geological Survey,
Keyworth, Nottingham NG12 5GG, UK
e-mail: pbw@bgs.ac.uk
tel: +44 (0) 115 936 3086
fax: +44 (0) 115 936 3261